Inorganic Chemistry

Article

Cite This: Inorg. Chem. 2018, 57, 10846−10856

pubs.acs.org/IC

Versatile Coordination and C−C Coupling of Diphosphine-Tethered Imine Ligands with Ni(II) and Ni(0)

Dide G. A. Verhoeven,[†] Hidde A. Negenman,[†] Alessio F. Orsino,[†] Martin Lutz,[‡] and Marc-Etienne Moret*,[†]

[†]Organic Chemistry and Catalysis, Debye Institute for Nanomaterials Science, Faculty of Science, Utrecht University, Universiteitsweg 99, 3584 CG, Utrecht, The Netherlands

[‡]Crystal and Structural Chemistry, Bijvoet Center for Biomolecular Research, Faculty of Science, Utrecht University, Padualaan 8, 3584 CH, Utrecht, The Netherlands

Supporting Information

ABSTRACT: Ligands that can adapt their coordination mode to the electronic properties of a metal center are of interest to support catalysis or small molecule activation processes. In this context, the ability of imine moieties to bind in either an η^1(N)-fashion via σ-donation of the lone pair or, less commonly, in an η^2(C,N)-fashion via π-coordination is potentially attractive for the design of new metal−ligand cooperative systems. Herein, the coordination chemistry of chelating ligands with a diphosphine imine framework (PCNP) to nickel is investigated. The imine moiety binds in an η^1(N)-fashion in a Ni(II)Cl_2 complex. The uncommon η^2(C,N)-interaction is obtained in Ni(0) complexes in the presence of a PPh_3 coligand. Increasing the bulk on the phosphine side-arms in the Ni(0) complexes, by substituting phenyl for *o*-tolyl groups, leads to a distinct binding mode in which only one of the phosphorus atoms is coordinated. In the absence of a coligand, a mixture of two different dimeric Ni(0) complexes is formed. In one of them, the imine adopts an uncommon η^1(N)η^2(C,N) bridging mode of the ligand to nickel, while the second one may involve reactivity on the ligand by the formation of a new C−C bond by oxidative coupling. The latter is supported by the isolation and structural characterization of a crystalline bis-CO derivative featuring a C−C bond formed by oxidative coupling of two imine moieties.

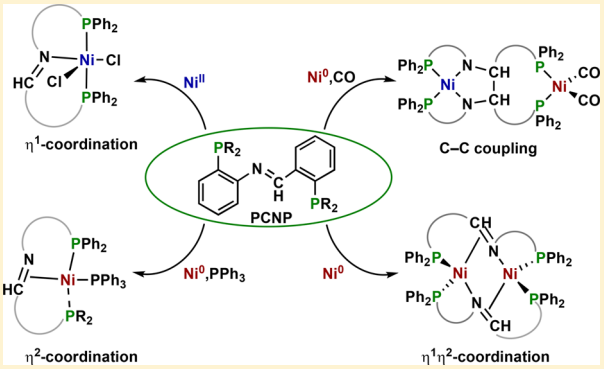

INTRODUCTION

In light of the ongoing interest in the substitution of precious metals by earth abundant metals in catalysis, the development of systems displaying metal−ligand cooperativity is flourishing.[1−4] Cooperative ligands can stabilize the metal center upon structural and electronic changes during catalytic processes by either adapting their binding mode or by reversibly accepting electrons, protons, or substrate fragments. For this purpose, ligands with versatile binding modes, facilitating hemilabile or adaptive behavior, or with the possibility of stabilizing multielectron redox processes, are of interest. In particular, π-ligands such as C═C double bonds have been shown to act as hemilabile ligands.[5] In this context, C═E (E = O, N) double bonds could constitute an attractive element of ligand design because of their ability to bind either through the E-centered lone pair or through the C═E π-system. Building on this idea, we recently reported that the diphosphine ketone ligand of 2,2′-bis(diphenylphosphino)benzophenone (^{Ph}dpbp) can act as a hemilabile acceptor ligand: the ketone moiety does not bind to the M(II)Cl_2 fragment (M = Fe, Co, Ni) but binds in an η^2-fashion to M(I)Cl.[6,7]

Imine functionalities are prevalent as ligands in organometallic chemistry, which is reflected in their numerous applications in homogeneous catalysis.[8,9] Examples are the NNN-pincer Fe and Co complexes independently reported by Gibson[10] and Brookhart[11] for alkene polymerization and investigated subsequently by Chirik for various reactions capitalizing on the redox noninnocent character of the imine moieties,[12] dinuclear Ni complexes as published by Uyeda that catalyze hydrosilylation reactions,[9j] or diphosphine imine complexes, reported by several groups, for olefin polymerization and oligomerization.[13−16] Generally, the imine nitrogen atom is reported to bind the metal center via its lone pair in an η^1(N)-fashion, forming a σ dative bond. A second, and less common, possibility is formation of π-complexes via an η^2(C,N)-coordination of the imine. This latter binding mode can be described by the Dewar-Chatt-Duncanson (DCD) model for coordination of π-ligands, i.e. the side-on bound and the metallo-aza-cycle extreme. Limited examples of an η^2(C,N)-bound benzophenone-imine to Ni(0) are reported,[17]

Received: May 30, 2018
Published: August 16, 2018

as well as a recently published bimetallic Ni complex with a chelating NNN-bis(imino)pyridine ligand.[18] Monometallic complexes with a chelating ligand with an η^2(C,N)-coordinating imine functionality based on precious metals Pd, Rh, and Ir are described as well.[19−24]

Here, we investigate the versatile binding of an imine ligand flanked by two *ortho*-diphenylphosphino-substituted phenyl rings to nickel. The design of the ligand allows for a chelated binding structure via the phosphine arms to the metal center. Synthesis of the diphosphine-imine ligand $P^{Ph}CNP^{Ph}$ (**1**, Scheme 1) and its complexation to Co(II),[13,14] Ni(II),[13,15]

Scheme 1. Synthesis of P^RCNP^R Ligand 1

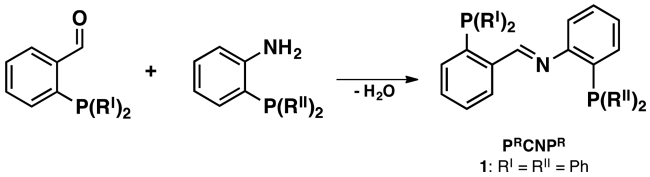

and Pd(II)[14,15] with the imine backbone bound in an η^1(N)-fashion has been reported previously, mainly for use in olefin oligomerization and polymerization reactions. In this contribution, the coordination chemistry of PCNP ligands to nickel is investigated, showing that the imine moiety is able to adopt a variety of coordination modes (end-on, side-on, bridging), changing upon varying the oxidation state from Ni(II) to Ni(0) and upon the addition of steric bulk on the phosphine tethers. Of particular interest is the observation of an oxidative C−C coupling reaction in dimeric complexes, in which a Ni(0)Ni(0) core is oxidized to Ni(II)Ni(0).

■ RESULTS AND DISCUSSION

The diphosphine-imine ligand $P^{Ph}CNP^{Ph}$ (**1**) was readily synthesized via an imine condensation of the diphenylphosphine substituted aldehyde and amine compounds (Scheme 1).[15,25] A Ni(II) complex was synthesized from reaction of $NiCl_2$(DME) with $P^{Ph}CNP^{Ph}$ in CH_2Cl_2, resulting in Ni($P^{Ph}CNP^{Ph}$)Cl_2 (**2**) after isolation via precipitation from THF/hexanes and extraction of the product (Scheme 2).[13] Analysis by ^{1}H NMR spectroscopy at room temperature showed the formation of a paramagnetic species, with broad aromatic peaks in the region of δ 6 to 9, and one largely shifted broad peak at δ 35.1. Upon lowering the temperature to −80 °C, the peaks sharpen, and the peak at δ 35.1 shifts to δ 8.9, suggesting a spin transition. The latter possibly involves a high spin tetrahedral structure at room temperature−where one chloride anion is dissociated−converting to a diamagnetic low spin square planar structure at low temperature (Supporting Information, Figures S4, S5). X-ray crystal structure determination of crystals grown by slow vapor diffusion of hexanes into CH_2Cl_2 showed that **2** has a strongly distorted square pyramidal geometry around nickel (Figure 1). The $P^{Ph}CNP^{Ph}$ ligand is bound via both phosphorus atoms and the imine moiety in an η^1(N)-fashion. The $P^{Ph}CNP^{Ph}$ ligand is disordered by a 180° rotation around the imine bond in a ratio 0.550(6):0.450(6) (see the Supporting Information). Next to this, two chloride ligands are bound, of which the apical Ni−Cl bond is strongly elongated to 2.6545(6) Å, versus 2.1889(5) Å for the in-plane chloride ligand. Hence, the geometry can be seen as derived from a cationic square-planar Ni(II) complex weakly interacting with a Cl^- counterion. This geometry is similar to that of the dibromide analogue of **2**, as published by Sun and co-workers, with Ni−Br bond lengths of 2.3222(11) Å for the in-plane Br and 2.7754(11) Å for the apical Ni−Br bond.[13] Furthermore, Ni−P and Ni−N distances are similar for the Cl and Br analogues (**2**: Ni1−N1A: 1.963(3), Ni1−P1A: 2.1892(6), Ni1−P2A: 2.1837(6) Å (Table 1). **2Br**:[13] Ni−N: 1.956(6), Ni−P(N-side): 2.154(2), Ni−P(C-side): 2.1972(19) Å). The torsion angle for C−N═C−C is 175.4(6)°, indicating a slightly distorted flat configuration of the ligand backbone (close to 180°) and the largely sp^2 character of the imine-carbon atom.

An η^2(C,N)-coordination mode of the imine moiety was accessed by synthesis of a Ni(0) complex. Reaction of ligand **1** with Ni(cod)$_2$ (cod = 1,5-cyclooctadiene) in the presence of PPh_3 as coligand in THF afforded the Ni(0) complex Ni($P^{Ph}CNP^{Ph}$)(PPh_3) (**3**) as a dark red solid after precipitation from THF/hexanes. Analysis by NMR spectroscopy displays a diamagnetic species with three signals in the ^{31}P NMR spectrum: a sharp doublet at δ 29.5 and two broad signals at δ 6.3 and 44.1. The broadening is possibly caused by the presence of a small amount of coprecipitated free PPh_3, causing the spectrum to broaden by exchange of the coligand. The ^{31}P NMR signals sharpen both at −50 and 50 °C (Figure S7). The sharp low-temperature spectrum shows the splitting pattern and coupling constants for complex **3**, from which it is evident that the three ^{31}P nuclei couple with each other (δ 46.80 (d, J_{PP} = 41 Hz), 30.00 (d, J_{PP} = 28 Hz), 4.16 (dd, J_{PP} =

Scheme 2. Overview of the Ligands and Ni-Complexes

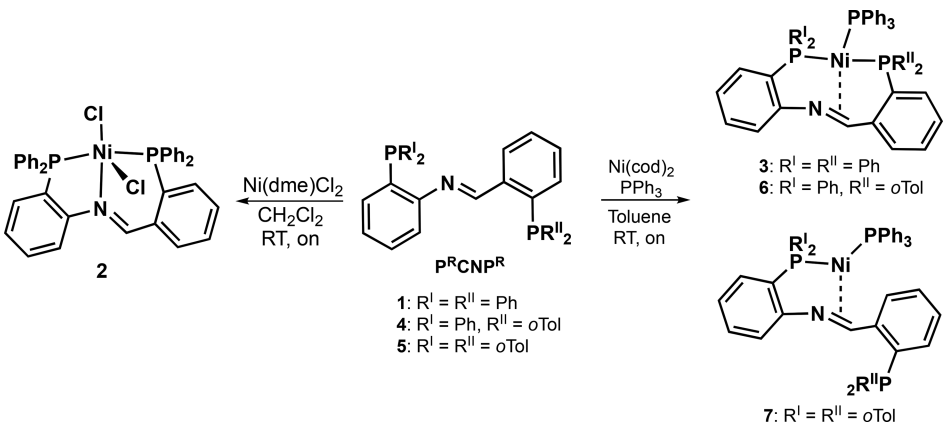

DOI: 10.1021/acs.inorgchem.8b01478
Inorg. Chem. 2018, 57, 10846−10856

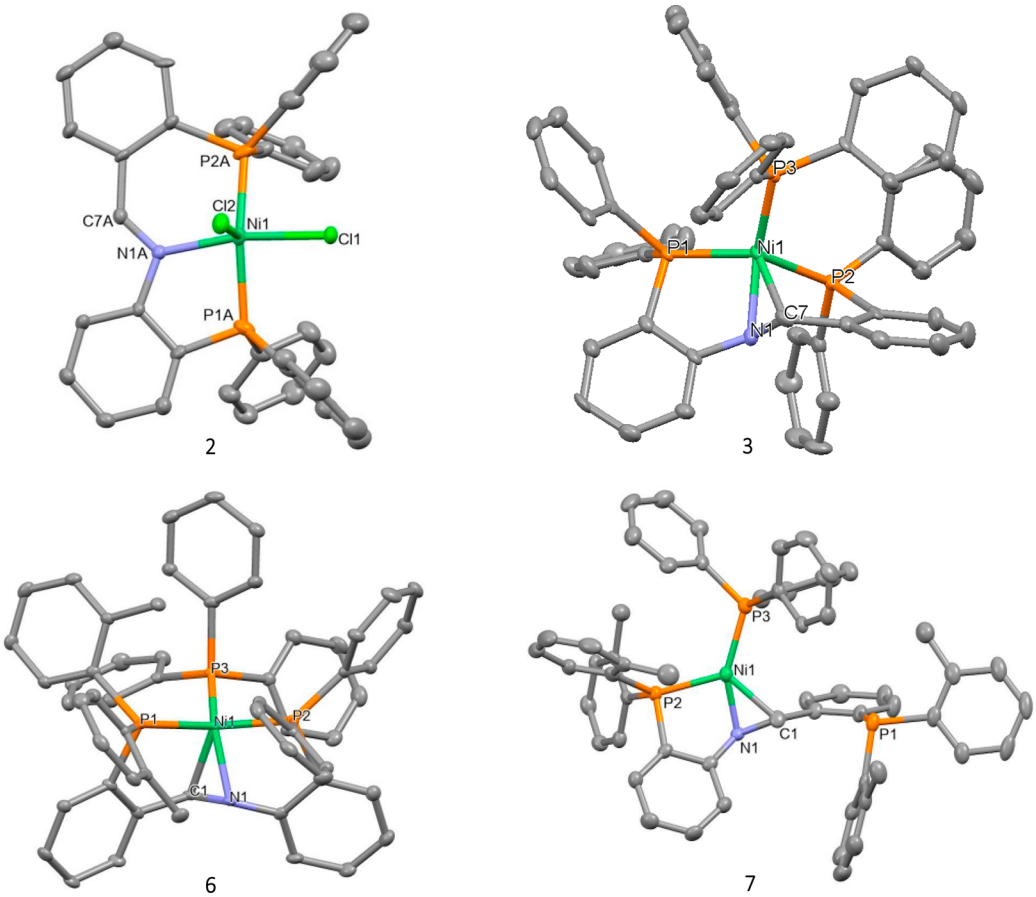

Figure 1. Molecular structures of **2**, **3**, **6**, and **7** in the crystal. Displacement ellipsoids are drawn at the 50% probability level. Cocrystallized solvent molecules and hydrogen atoms are omitted for clarity: **2**: 0.5 Et_2O and 0.5 CH_2Cl_2; **7**: THF. Selected distances (Å) and angles (deg): **2**: only the major disorder component of the structure is shown here. Ni1−N1A: 1.963(3), Ni1−C7A: 2.913(4), N1A−C7A: 1.294(5), Ni1−P1A: 2.1892(6), Ni1−P2A: 2.1837(6), Ni1−Cl1: 2.1889(5), Ni1−Cl2: 2.6545(6), P1A−Ni1−P2A: 153.13(3), Cl1−Ni1−N1A: 169.69(10). **3**: Ni1−N1: 1.943(3), Ni1−C7: 2.075(4), N1−C7: 1.364(5), Ni1−P1: 2.1888(11), Ni1−P2: 2.3234(11), Ni1−P3: 2.1761(11), P1−Ni1−P2: 121.89(4). **6**: Ni1−N1: 1.969(2), Ni1−C1: 2.031(3), N1−C1: 1.358(4), Ni1−P1: 2.2996(8), Ni1−P2: 2.2189(8), Ni1−P3: 2.1904(9). **7**: Ni1−N1: 1.864(3), Ni1−C1: 2.044(4), N1−C1: 1.368(4), Ni1−P1: 4.8493(12), Ni1−P2: 2.2048(11), Ni1−P3: 2.1475(12).

Table 1. Selected Bond Distances (Å) and Angles (deg) in the X-ray Crystal Structures[b]

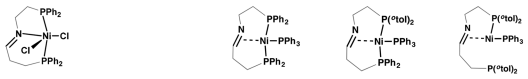

	2a	2b	3	6	7
C–N	1.294(5)	1.287(6)	1.364(5)	1.358(4)	1.368(4)
Ni–C	2.913(4)	2.886(4)	2.075(4)	2.031(3)	2.044(4)
Ni–N	1.963(3)	1.968(4)	1.943(3)	1.969(2)	1.864(3)
Ni–PPh_3	-	-	2.1761(11)	2.1904(9)	2.1475(12)
Ni–$P_{(N)}$	2.1892(6)[a]	2.1837(6)[a]	2.1888(11)	2.2189(8)	2.2048(11)
Ni–$P_{(C)}$	2.1837(6)[a]	2.1892(6)[a]	2.3234(11)	2.2996(8)	4.8493(12)
Torsion angle C–C–N–C	175.4(6)	–179.0(7)	151.4(3)	147.0(3)	145.8(3)

[a]Constraints were used for the P atoms in the two disorder components. [b]**2a** is the major and **2b** is the minor disorder component of complex **2**. For clarity, the phenylene linkers in all structures are represented with gray lines.

28, 41 Hz)). Free PPh_3 is not observed in this spectrum, which is probably due to its low concentration. The free imine is no longer present in **3**, as the distinctive imine−CH peak in the ^{1}H NMR spectrum at δ 9.32 in **1** is not observed, nor is the C═N band in IR analysis.[26] ^{1}H−^{13}C HMQC 2D NMR analysis shows a cross peak for a signal at δ 84 in ^{13}C NMR and δ 6 in ^{1}H NMR spectrum, which is assigned to the imine−CH moiety (Figure S8). The considerable shift of the ^{13}C NMR signal toward high field is indicative of a strong rehybridization toward sp^3, i.e. a substantial metallacycle character of the M−C−N unit. It is, however, somewhat smaller than that observed in tricoordinate aldimine complexes of the (dippe)Ni fragment (dippe = bis-(diisopropylphosphino)ethane),[17d] in which this signal is found at ca. δ 60. This difference likely arises from more efficient π-backdonation from the (Ni−P) σ-antibonding in-plane d-orbital in tricoordinate complexes. Crystallographic analysis of **3** showed a distorted tetrahedral geometry around the nickel center (Figure 1).[27] The Ni(0) center is bound to **1** in a κ^4(P,P,C,N)-fashion with an η^2(C,N)-coordination of the imine backbone and to the PPh_3 coligand. The C−N distance of the imine moiety is clearly larger in **3** (1.364(5) Å) than in the Ni(II) complex **2** (1.294(5) Å), as a result of π-backdonation to the antibonding π^* orbital of the imine C═N bond.

Ligand Variation. The design of the ligand allows for facile incorporation of different substituents on phosphorus, including mixed ligands, as the building blocks of the imine

DOI: 10.1021/acs.inorgchem.8b01478
Inorg. Chem. 2018, 57, 10846−10856

Scheme 3. Synthesis of Dimeric Complexes Derived from 1[a]

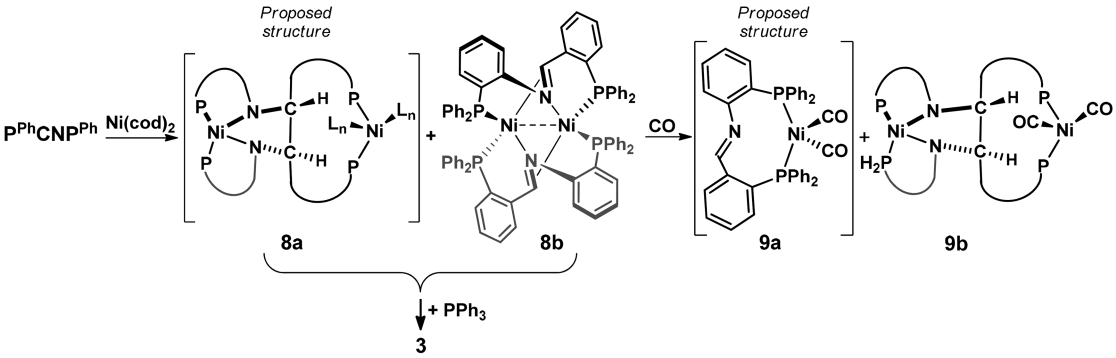

[a]P = PPh_2, L is a solvent molecule.

condensation can be adjusted. The influence of additional bulk on the $P^{R}CNP^{R}$ ligand was explored by the synthesis of the *o*-tolyl substituted ligands (Scheme 2). The ligands $P^{Ph}CNP^{oTol}$ (**4**) and $P^{oTol}CNP^{oTol}$ (**5**) were synthesized accordingly, and subsequent complexation via a reaction of the ligand with $Ni(cod)_2$ and PPh_3 in toluene afforded Ni(0) complexes $Ni(P^{Ph}CNP^{oTol})(PPh_3)$ (**6**) and $Ni(P^{oTol}CNP^{oTol})(PPh_3)$ (**7**), respectively, after precipitation with hexanes and isolation of the solids.

Complex **6** gives rise to three broad signals in the ^{31}P NMR spectrum at δ 36, 29, and 1, all in the region of nickel bound phosphorus compounds. The broad signals suggest fluxionality in the complex, which is assumed to be caused by the increased bulk. ^{1}H NMR indicates a shift of the imine-CH moiety as the distinctive imine-proton (δ 9.33 in **4**) is no longer present. The X-ray crystal structure on single crystals grown from vapor diffusion of hexane into THF showed a tetrahedral configuration around the nickel center, bound to PPh_3, and **4** in a κ^4(P,P,C,N)-fashion with an η^2(C,N)-coordination of the imine backbone (Figure 1). The imine C−N distance is 1.358(4) Å, which is similar to that in complex **3** (Table 1). Likewise, the Ni−P distances closely resemble the analogues distances of complex **3**.

The bulkier substituents on the phosphorus atoms in the tetra-*ortho*-tolyl PCNP ligand **5** and its nickel complex **7** result in decoordination of one of the phosphine arms: the ^{31}P NMR spectrum of **7** shows again three signals, but in this case one peak appears as a broad singlet at δ −28, indicating a noncoordinated phosphorus atom. The remaining two signals—also broad singlets—are found at δ 11 and 40, consistent with coordination to Ni. Single crystal X-ray structure determination confirms this interpretation: nickel is bound to the ligand in a κ^3(P,C,N)-fashion with an η^2(C,N)-coordination of the imine moiety (Figure 1). Next to this, PPh_3 is bound, and the carbon-side phosphine of the PCNP ligand is dissociated. The imine C−N bond length is 1.368(4) Å for **7**, which is comparable to the elongation of the imine backbone in **3** and **6**, indicating a similar degree of π-backbonding despite the lower coordination number. The Ni−N bond distance of 1.864(3) Å is however shorter compared to **3** and **6**, which is likely caused by the lesser amount of geometric strain due to the detachment of the second phosphine arm. The torsion angle C−N═C−C for **3**, **6**, and **7** is similar, with 151.4(3)° for **3**, 147.0(3)° for **6**, and 145.8(3)° for **7**. These angles differ from an sp^2 (180°) and an sp^3 (120°), consistent with an intermediate hybridization, with a slightly higher degree of sp^3 character for **7**.

Dimeric Complexes. Reaction of **1** and $Ni(cod)_2$ in toluene without the addition of a coligand resulted in a mixture of two species, major species **8a** and minor species **8b** (Scheme 3). A workup was performed by precipitation of the products upon addition of hexanes to a THF solution, removing the majority of cod in the filtrate, followed by extraction of the solids in THF and evaporation of the solvent in vacuum and remaining cod by high vacuum.[28] The mixture mainly consists of **8a**, allowing for its spectroscopic characterization, which shows the absence of a free imine moiety, as the imine-hydrogen peak is shifted in ^{1}H NMR and the according band in the IR spectrum at 1621 cm^{-1} is not observed.[26] Four signals are observed in the ^{31}P NMR spectrum: two doublets at δ 35.4 and −7.9 (J_{PP} = 9 and J_{PP} = 70 Hz) and two double−doublets at δ 35.5 and 22.9 (J_{PP} = 2, 70 and J_{PP} = 2, 9 Hz). This indicates that the four nonequivalent phosphorus atoms belong to a single product, which is likely to be caused by a dimeric nature of **8a**. Heating a sample of **8a**/**8b** up to 100 °C did not reveal exchange of the four inequivalent ^{31}P signals of **8a** on the NMR time scale (Figure S39). Next to **8a**, the minor species **8b** is present in approximately 10 to 20%, which shows two doublet signals in the ^{31}P NMR spectrum at δ 1.1 and 38.3 (J_{PP} = 43 Hz). No conditions could be identified that would allow for bulk isolation of either **8a** or **8b**, but the ratio between the species appears to be somewhat sensitive to the conditions of precipitation (see below), suggesting that **8a** and **8b** are kinetic products that have not reached equilibrium. To establish the overall composition of the mixture, one equivalent of PPh_3 with respect to nickel was added. Quantitative conversion of **8a**/**8b** into **3** was observed, confirming the overall composition of $[Ni(P^{Ph}CNP^{Ph})]_{2n}$ (Scheme 3) and demonstrating the synthetic use of the mixture as a source of the $[Ni(P^{Ph}CNP^{Ph})]$ fragment.

Diffusion of hexanes into a THF solution afforded crystals suitable for X-ray diffraction, although only a minor fraction of the material crystallized. The crystalline material was covered by precipitation of a second compound, preventing bulk isolation. An NMR spectrum of the solid materials revealed a mixture of **8a** and **8b** (about 1:1), showing the increasing presence of the minor species after crystallization. A crystal could be harvested from the mixture and subjected to X-ray diffraction. The obtained crystal structure presents a dimeric species with two ligands and two nickel centers, identified as the minor component **8b** (Figure 2): even though no

DOI: 10.1021/acs.inorgchem.8b01478
Inorg. Chem. 2018, 57, 10846−10856

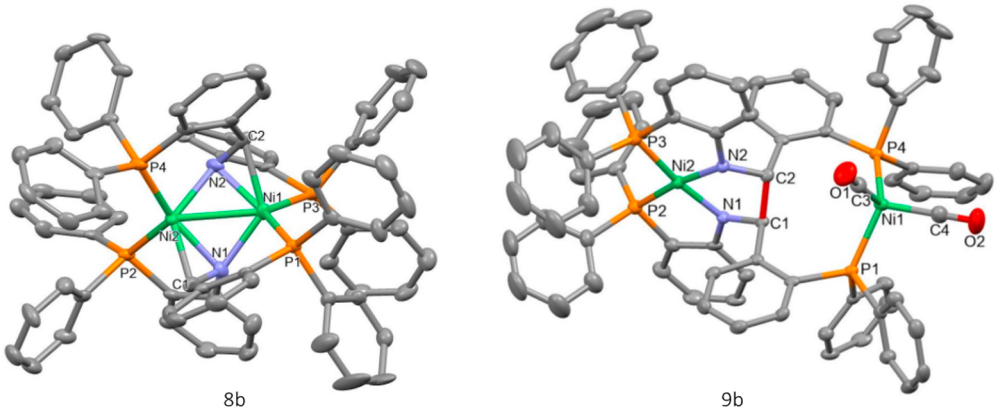

Figure 2. Molecular structures of **8b** and **9b** in the crystal. Displacement ellipsoids are drawn at the 50% probability level, and hydrogen atoms are omitted for clarity. Selected distances (Å) and angles (deg): **8b**: N1−C1: 1.347(6), N2−C2: 1.361(6), N1−Ni1: 2.033(4), N1−Ni2: 1.992(4), N2−Ni1: 2.004(4), N2−Ni2: 2.031(4), Ni1−Ni2: 2.5595(9), Ni1−C2: 2.063(5), Ni2−C1: 2.046(5). **9b**: Formed C1−C2 bond is shown in **red**. C1−C2: 1.550(4), N1−C1: 1.448(4), N2−C2: 1.460(4), Ni2−P2: 2.1545(10), Ni2−P3: 2.1529(10), Ni2−N1: 1.884(3), Ni2−N2: 1.884(3), Ni1−P1: 2.2228(9), Ni1−P4: 2.2269(9), Ni1−C3: 1.765(4), Ni1−C4: 1.774(4).

crystallographic symmetry is found, the overall structure of **8b** possesses an approximate 2-fold rotation axis perpendicular to the Ni−Ni axis, which suggests that its ^{31}P NMR spectrum should display only two signals. Each imine moiety acts as a bridge, binding side-on to one metal and end-on to the other, with the two P-donor sites of one ligand binding each to a different Ni center. The structure has a rather short Ni−Ni distance of 2.5595(3) Å which is likely sterically enforced by the geometrical arrangement of the ligands. An electronic Ni−Ni interaction is unlikely because both centers possess a d^{10} configuration. The C═N bond distances in **8b** are 1.347(6) Å and 1.361(6) Å, both comparable to the monomeric Ni(0) complexes discussed above; thus, the additional σ(N)-interaction does not seem to contribute significantly to a more activated imine.

The somewhat unusual μ−η^1(N)η^2(C,N) binding mode observed in **8b** has been previously reported by de Bruin and co-workers in dinuclear rhodium(I) complexes formed by deprotonation of the α-CH_2 group of a bridging dipicolylamine (dpa) ligand (Figure 3).[19] Subsequent work by the same group

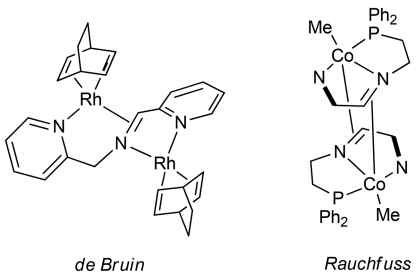

Figure 3. Complexes by de Bruin and Rauchfuss. The bold line in the right drawing represents a pyridine ring of which only the bound C−N is shown.

has afforded a number of related (hetero)bimetallic compounds featuring the same binding mode, which could also be accessed directly from the imine analogue of the ligand (dpi).[21−23] Very recently, a similar Co^I_2(imine)$_2$ core was observed by Rauchfuss and co-workers in the dimer [CoMe($^{Ph2}P^{C2}N^{H}$py)]$_2$, where $^{Ph2}P^{C2}N^{H}$py is a tridentate pyridine-imine-phosphine (pyCNP) ligand, differing from the PCNP framework by substitution of the second *o*-diphosphinophenylene linker by a pyridine group (Figure 3).[29] Notably, the Co−Co distance of ca. 2.9 Å is considerably longer than the Ni−Ni distance of 2.5595(9) Å in **8b**, which is likely a result of the different local coordination geometry: 5-coordinate, trigonal bipyramidal (TBP) for Co^I vs tetracoordinate, tetrahedral for Ni^0.

The chemical nature of major dimeric species **8a** could not be fully elucidated. Further analysis of the mixture shows the presence of two distinctive signals in the ^{1}H NMR spectrum at δ 4.58 and 5.49 that belong to the major species **8a**, besides numerous aromatic signals. Even though the low solubility of the compound leads to a low quality ^{13}C NMR spectrum, the ^{1}H−^{13}C HMQC NMR spectrum shows clear cross peaks with ^{13}C NMR signals at δ 78.7 and 86.90, respectively, which are both shown to be CH signals, according to APT ^{13}C NMR analysis (Figures S35, S38). A possible explanation is the incorporation of a new C−C bond in the species. The absence of a large $^3J_{HH}$ between these two signals would then be due to a constrained H−C−C−H dihedral angle in the low-coupling Karplus region.[30] Upon arrangement of two imine bonds in close proximity to each other, possibly in the form of a dimer, the imine-carbon atoms can undergo a coupling reaction in which two electrons from a metal center are transferred to the ligand, forming a new carbon−carbon bond (Scheme 3). A similar reaction was reported by Rauchfuss and co-workers,[31] where the coupling of two imine moieties from diphenylphosphino-2-benzimine ligands bound to iron(0) undergoes a coupling reaction upon addition of ferrocenium, analogous to a pinacol coupling observed on iron(0) in their earlier research.[32−35] However, it should be noted that a single dimeric molecule with two inequivalent η^2(C,N)-coordinating imine moieties cannot be excluded on the basis of the obtained data, since a shift around δ 5 in the ^{1}H NMR spectrum and δ 80 in the ^{13}C NMR spectrum could also correspond to such a structure.[17d]

Evidence supporting the structure containing a new C−C bond arises from the reactivity of the **8a**/**8b** mixture with CO. A solution of **8a**/**8b** in C_6D_6 was exposed to CO (1 atm), after which the mixture was monitored in situ by NMR spectroscopy. ^{31}P NMR data shows the formation of two species: major species **9a** with two doublet signals at δ 33.0 and 16.2 (J_{PP} = 11 Hz) and minor species **9b** with two singlet signals at δ 39.8 and

DOI: 10.1021/acs.inorgchem.8b01478
Inorg. Chem. 2018, 57, 10846−10856

22.1 (approximate ratio of 3.3:1) (Figure S42). Crystallization by slow vapor diffusion of hexanes into a benzene mixture resulted in single crystals of the minor product **9b** (Figure 2, Scheme 3). The X-ray crystal structure shows a dimeric, mixed valence Ni(0)Ni(II) complex with two added equivalents of CO both bound to the Ni(0) center. The Ni(II) center is surrounded by two neutral phosphine ligands and two anionic amido (R_2N^-) ligands, an uncommon coordination environment that was also observed in the Ni(II) complex of the P_2N_2 ligand *N*,*N*′-bis[2-(diphenylphosphino)phenyl]propane-1,3-diamine published by Duckworth, McPartlin, and co-workers.[34] Compared to Ni(II) complex **2**, the Ni−N bonds are rather short, 1.963(3) Å in **2** (major disorder component) and 1.884(3) Å and 1.884(3) Å in **9b**, originating from the strong π-donating nature of the nitrogen ligands. Noteworthy, the C−H hydrogen bound to C2 in the formed C−C bond has a rather short distance below 3 Å to the Ni(0) center. This is, however, attributed to the rigid geometry of the structure rather than a chemical interaction.

Crystals of **9b** could be isolated from the **9a**/**9b** mixture and were analyzed by NMR. ^{31}P NMR analysis indeed shows the signals earlier attributed to **9b**, without the presence of other species, and the ^{1}H NMR spectrum shows a number of aromatic signals located in the range of δ 5.94 to 10.09. The large shift of the aromatic signals was confirmed by ^{1}H−^{13}C HMQC 2D NMR analysis, as coupling signals are observed for these peaks with the aromatic region of the ^{13}C NMR spectrum. The exception is a broad singlet signal at δ 6.18, which has a coupling signal in the ^{13}C NMR spectrum at δ 70.35 and is identified as the amido−CH functionality of the formed C−C bond. Furthermore, 2D ^{1}H−^{31}P HMBC NMR analysis shows a coupling with both phosphorus substituents of this proton (Figure S45). The IR spectrum of the crystals contains two signals for the CO bands at 1938 and 1999 cm^{-1}. Complex **9b** contains two Ni-centers, in two oxidation states, i.e. the Ni(0) and Ni(II) center. The formal oxidation state of the Ni(0) center is unchanged, starting from the Ni(0) precursor $Ni(cod)_2$. The Ni(II) center, on the other hand, was formed via an intramolecular redox process, by transfer of its electrons to the formed C−C bond originating from the imine moieties (Scheme 3).

The isolated compound **9b** is however not the major species in the reaction mixture. The majority of the material (**9a**) shows two intense CO signals in the IR spectrum at 1929 and 1991 cm^{-1}, slightly shifted from the CO signals in **9b**, and NMR analysis shows the presence of aromatic signals in the ^{1}H and ^{13}C NMR spectra. In addition, the ^{1}H−^{13}C HMQC 2D NMR spectrum shows a coupling signal for a peak at δ 7.8 in ^{1}H NMR and δ 155 in ^{13}C NMR consistent with a noncoordinating imine-CH, which suggests the monomeric structure depicted in Scheme 3 for compound **9a**. More complex, possibly oligomeric structures can however not be fully excluded.

Combining the obtained data of compounds **8a**, **8b** and **9a**, **9b** suggests that the CO ligands act here as a trapping agent for the structure with the C−C bond, **8a**, making its isolation possible. In the case of **8a**, solvent molecules such as THF are likely coordinating to the Ni(0) center, which upon dissolution in benzene could be replaced by a benzene molecule.[36] Isolation is facilitated by replacing loosely bound solvents for stronger binding CO ligands, resulting in **9b**. The higher apparent symmetry of **9b** (two ^{31}P NMR signals) with respect to **8a** (four ^{31}P NMR signals) may be due to higher fluxionality of the Ni(0) center in **9b**. The formation of the interligand C−C bond by a two-electron transfer from the metal to the ligand resulting in **8a** and **9b** shows the possibility of the PCNP ligand to engage into ligand-centered redox processes, possibly opening new venues for cooperative processes besides the versatile binding as observed in complexes **2**, **3**, **6**, and **7**. Interestingly, the fact that the mixture **8a**/**8b** can be quantitatively converted to the imine complex **3** by addition of PPh_3 suggests that C−C bond formation may be reversible. These properties make Ni(PCNP)-complexes potentially interesting candidates for cooperative activation of substrates and subsequent catalysis. Further reactivity of these complexes is currently under investigation in our laboratories.

■ CONCLUSIONS

The coordination chemistry of chelating diphosphine-imine P^RCNP^R ligands to nickel was studied. The potential adaptive behavior of the phenyl-substituted ligand is exemplified in its coordination to Ni(II) and Ni(0): the imine moiety binds in an η^1(N) fashion to Ni(II) and in an η^2(C,N) fashion to the more electron-rich Ni(0). The addition of steric bulk to the P^RCNP^R framework in the form of *o*-tolyl substituents on the phosphorus atoms affords mixed-ligand complex **6**, where both phosphine tethers of the $P^{oTol}CNP^{Ph}$ ligand are bound to nickel, and tetra-*o*-tolyl ligand complex **7**, where one phosphine arm is dissociated from the metal center. When no coligand is used in the synthesis of the Ni(0) complex with the $P^{Ph}CNP^{Ph}$ ligand, a mixture of dimeric structures is obtained, with a) an η^1(N)η^2(C,N)-coordination of the two imine ligands to both Ni centers as shown by its X-ray crystal structure and b) a complex in which the imine functionalities seem to undergo a coupling reaction forming a new C−C bond. Addition of CO to the mixture leads to the isolation of a derivative of the C−C bound complex. The current study provides detailed insight into the coordination of η^2(C,N)-bonding imine ligands to nickel, which are becoming prolific tools in the field of metal−ligand cooperativity. The observed adaptive behavior of the ligand upon different oxidation states and the redox-activity of the dimeric species make these complexes highly interesting for investigation toward their cooperative reactivity and catalytic activity. Further reactivity of these complexes is currently under investigation in our laboratories.

■ EXPERIMENTAL SECTION

General Considerations. All reagents were purchased from commercial sources and used as received unless stated otherwise. All reactions were performed under N_2 using standard Schlenk and glovebox techniques unless stated otherwise. Deuterated benzene (C_6D_6) and deuterated dichloromethane (CD_2Cl_2) were degassed using the freeze−thaw−pump method (4×) and subsequently stored over molecular sieves. Dichloromethane (CH_2Cl_2) was distilled over calcium hydride, and tetrahydrofuran (THF) was distilled over sodium/benzophenone before use; both were degassed by bubbling N_2 through it for 30 min and stored over molecular sieves. Dry diethyl ether (Et_2O), hexanes, acetonitrile (MeCN), and toluene were acquired from a MBRAUN MB SPS-80 solvent purification system and further dried over molecular sieves before use. MeCN was filtered over alumina prior to use. 2-Diphenylphosphanyl-benzaldehyde[37−39] and 2-diphenylphosphinoaniline[40] were synthesized according to literature procedures.

^{1}H, ^{13}C, and ^{31}P NMR spectra (respectively 400, 100, and 161 MHz) were recorded on an Agilent MRF400 or a Varian AS400 spectrometer at 25 °C. ^{1}H and ^{13}C NMR chemical shifts are reported

DOI: 10.1021/acs.inorgchem.8b01478
Inorg. Chem. 2018, 57, 10846−10856

in ppm relative to TMS using the residual solvent resonance as internal standard. ^{31}P NMR chemical shifts are reported in ppm and externally referenced to 85% aqueous H_3PO_4. Infrared spectra were recorded using a PerkinElmer Spectrum One FT-IR spectrometer equipped with a general liquid cell accessory under a N_2 flow. ESI-MS spectra were recorded on a Walters LCT Premier XE KE317 Micromass Technologies spectrometer. Compounds of which elemental analysis is reported were either recrystallized or precipitated and dried under high vacuum overnight before submission, and analysis was performed by the Mikroanalytisches Laboratorium Kolbe, Mülheim an der Ruhr, Germany.

*2-Ph$_2$PC$_6$H$_4$N═C(H)C$_6$H$_4$PPh$_2$ (P^{Ph}CNP^{Ph}, **1**).* This was adapted from a literature procedure.[15] 2-Diphenylphosphinobenzaldehyde (6.0 g, 0.021 mol), 2-diphenylphosphinoaniline (5.73 g, 0.021 mol), and *p*-toluene sulfonic acid (0.11 g, 0.58 mmol) were dissolved in toluene (500 mL) in a 3-necked round-bottom flask under an N_2 atmosphere. A Dean−Stark trap was attached, and the collecting end was filled with molecular sieves (4 Å). The brown solution was heated to reflux for 17 h, after which all solvents were evaporated. The product was precipitated from a DCM/MeOH mixture, after which the solids were collected and washed with MeOH until the supernatant was colorless. Drying of the yellow solid resulted in the product with a yield of 60% (6.94 g, 0.013 mol). ^{1}H NMR: δ_H 9.32 (d, J = 6 Hz, 1H, −N═C*H*−), 8.39 (dd, J = 4, 4 Hz, 1H, Ar−*H*), 7.45 (t, J = 7 Hz, 4H, Ar−*H*), 7.28 (m, 4H, Ar−*H*), 6.93−7.02 (m, 16H, Ar−*H*), 6.82−6.89 (m, 2H, Ar−*H*), 6.58 (dd, J = 3, 5 Hz, 1H, Ar−*H*) ppm. ^{13}C NMR: δ_C 158.15 (dd, J_{CP} = 2.0, 24.0 Hz), 155.04 (d, J_{CP} = 18.1 Hz), 140.09 (d, J_{CP} = 17.55 Hz), 138.67 (d, J_{CP} = 19.3 Hz), 138.16 (d, J_{CP} = 13.7 Hz), 136.89 (d, J_{CP} = 11.1 Hz), 134.5 (dd, J_{CP} = 2.6, 18.2 Hz), 133.63 (d, J_{CP} = 13.8 Hz), 133.29 (d, J_{CP} = 33.4 Hz), 131.15, 130.09, 129.29, 129.12, 129.01 (d, J_{CP} = 7.0 Hz), 128.70, 128.63, 126.29, 117.50 ppm. ^{31}P NMR: δ_P −13.5, −14.9 ppm. IR: 3054, 1621, 1561, 1465, 1432, 1358, 1309, 1263, 1189, 1157, 1090, 1069, 1026, 999, 751, 738, 695, 499, 409 cm^{-1}. ESI-MS (MeCN/formic acid) m/z: [M + H]$^+$ calcd: 550.1854, Found: 550.1780.

*Ni(PCNP)Cl$_2$ (**2**).* P^{Ph}CNP^{Ph} (**1**) (499 mg, 0.908 mmol) was dissolved in CH_2Cl_2 (2 mL). A solution of $NiCl_2$(DME) (199.9 mg, 0.910 mmol) in CH_2Cl_2 (8 mL) was added, after which the color of the mixture turned from a bright yellow suspension to a yellow/brown solution. The mixture was stirred for 3 h 15 min, after which all solvents were removed in vacuum. The remaining solids were dissolved in a minimum amount of THF, and addition of hexanes caused precipitation. The solids were filtered off and collected via filtration with CH_2Cl_2. The product was obtained as a brown solid after evaporation of all solvents with a yield of 95% (0.584 g, 0.860 mmol). ^{1}H NMR (CD_2Cl_2): δ_H 35.09, 8.63, 8.22, 7.94, 7.88, 7.76, 7.10, 7.01, 6.91, 6.75, 6.28 ppm. ^{31}P and ^{13}C NMR: no signal detected. ESI-MS (MeCN) [M − Cl]$^+$ m/z: calcd: 642.0817, found: 642.0851. IR: 3051, 1585, 1572, 1223, 1481, 1434, 1309, 1280, 1182, 1155, 1096, 1067, 998, 766, 747, 729, 691, 575, 521, 501 cm^{-1}. Crystals for X-ray analysis were grown from CH_2Cl_2/hexanes. Elemental analysis, calcd: C 65.43, H 4.30, N 2.06, found: C 65.29, H 4.52, N 2.04.

*Ni(P^{Ph}CNP^{Ph})(PPh$_3$) (**3**).* P^{Ph}CNP^{Ph} (**1**) (200 mg, 0.364 mmol), PPh_3 (95.4 mg, 0.364 mmol), and Ni(COD)$_2$ (100.1 mg, 0.364 mmol) were combined in a vial, and Et_2O (9 mL) was added, resulting in a yellow-brown turbid mixture. The mixture was stirred for 5 h, in which the color changed to red-brown, after which the solvent was evaporated. THF (2 mL) was added to the solids, followed by addition of hexanes (6 mL) to precipitate the product as a red-brown solid, which was isolated via filtration and collected using THF. After evaporation of all solvents, **5** was obtained with a yield of 94% (299.3 mg, 0.344 mmol). ^{1}H NMR (C_6D_6) due to extended overlap between the signals and with the solvent, integrals could not be assigned: δ_H 7.79 (m, Ar−*H*), 7.49 (t, J = 8 Hz, Ar−*H*), 7.39 (s, broad, Ar−*H*), 7.35−7.19 (m, Ar−*H*), 7.08−6.61 (m, Ar−*H*), 6.00 (t, J = 5 Hz, Ar−*H*) ppm. ^{13}C NMR (C_6D_6): (note: precise assignment of signals hampered due to quality of the spectrum) δ_C 137.9, 137.5, 133.6, 133.5, 133.4, 133.2, 133.1, 132.9, 132.4, 132.2, 132.2, 132.0, 129.4, 128.2, 127.0, 125.1, 124.7, 120.4, 120.0, 99.6, 83.8 ppm. ^{31}P NMR (d_8-toluene, 25 °C): δ_P 44.1, 29.5, 6.1 ppm. ^{31}P NMR (d_8-toluene, −50 °C): δ_P 46.80 (d, J_{PP} = 41 Hz), 30.00 (d, J_{PP} = 28 Hz), 4.16 (d, J_{PP} = 28, 41 Hz) ppm. IR: 3050, 1574, 1554, 1477, 1455, 1432, 1398, 1313, 1179, 1152, 1113, 1089, 1027, 815, 739, 693, 502, 436, 417 cm^{-1}. Crystals for X-ray analysis were grown from THF/hexanes. The compound is too sensitive for transportation for elemental analysis.

2-Di-o-tolyl-phosphinoaniline. Triethylamine (0.25 mL, 1.79 mmol) was added to a solution of 2-iodoaniline (375 mg, 1.71 mmol) and di-*o*-tolyl-phosphine (365 mg, 1.70 mmol) in MeCN (9 mL) in a round-bottom flask under an N_2 atmosphere, to which subsequently a suspension of Pd(PPh$_3$)$_4$ (20.4 mg, 0.018 mmol) in H_2O/MeCN (12 mL, 1:2 ratio) was added. The pale orange mixture was refluxed for 64 h, after which all solvents were evaporated. Degassed CH_2Cl_2 (10 mL) was added, the organic layer was washed with degassed H_2O (3 × 10 mL) and collected, and the solvents were evaporated. The pale brown solid was washed with cold, degassed MeOH (3 × 4 mL) and dried in vacuum, resulting in the product as an off-white to pink solid with a yield of 87% (452.1 mg, 1.48 mmol). ^{1}H NMR (C_6D_6): δ_H 7.14 (m, 2H, Ar−*H*), 7.08−6.89 (m, 8H, Ar−*H*), 6.57, (t, J = 7 Hz, Ar−*H*), 6.32 (t, J = 7 Hz, Ar−*H*), 3.73 (s, 2H, −N*H*$_2$), 2.39 (s, 6H, −C*H*$_3$) ppm. ^{13}C NMR (C_6D_6): δ_C 151.10 (d, J_{CP} = 21 Hz), 142.80 (d, J_{CP} = 27 Hz), 135.11 (d, J_{CP} = 2 Hz), 134.19 (d, J_{CP} = 8 Hz), 133.26, 130.74, 130.58 (d, J_{CP} = 4 Hz), 129.13, 126.65, 117.10 (d, J_{CP} = 6 Hz), 115.32 (d, J_{CP} = 3 Hz), 21.32 (d, J_{CP} = 20 Hz) ppm. ^{31}P NMR (C_6D_6): δ_P −36.56 ppm. IR cm^{-1}: 3457, 3344, 3055, 3005, 1613, 1599, 1475, 1439, 1304, 1245, 1161, 1081, 1033, 799, 746, 717, 556, 517, 456. Elemental analysis: calcd: C 78.67, H 6.60, N 4.59; found: C 78.86, H 6.77, N 4.57. ESI-MS (MeCN/formic acid) m/z: calcd: 306.1412, found: 306.1478.

2-Di-o-tolyl-phosphinobenzaldehyde. The compound is reported in the literature,[39] but an adapted synthesis method was used. 2-Bromobenzaldehyde (3.00 mL, 0.476 g, 25.7 mmol), di-*o*-tolyl-phosphine (5.51 g, 25.7 mmol), and Pd(PPh$_3$)$_4$ (16.2 mg, 0.014 mmol) were dissolved in toluene (90 mL) in a round-bottom flask under an N_2 atmosphere, to which triethylamine (3.60 mL, 2.60 g, 25.8 mmol) was added. The orange suspension was refluxed for 8 h, after which the mixture was filtered, and washed with subsequently NH_4Cl (3 × 50 mL) and brine (1 × 50 mL). The solvents were removed in vacuum, and the remaining solids were washed with cold degassed MeOH (3 × 40 mL) and dried in vacuum, resulting in the product as an off-white solid to brown with a yield of 93% (7.65 g, 24.0 mmol). ^{1}H NMR (C_6D_6): δ_H 10.61 (d, J = 6 Hz, 1H, C*H*═O), 7.77 (ddd, J = 1, 3, 4 Hz, 1H, Ar−*H*), 7.06−6.84 (m, 11 H, Ar−*H*), 2.34 (s, 6H, −C*H*$_3$) ppm. ^{13}C NMR (C_6D_6): δ_C 190.62 (d, J_{CP} = 22 Hz), 143.02 (d, J_{CP} = 27 Hz), 140.02 (d, J_{CP} = 26 Hz), 139.61 (d, J_{CP} = 16 Hz), 135.03 (d, J_{CP} = 11 Hz), 134.17, 133.77, 133.54, 130.67 (d, J_{CP} = 5 Hz), 130.66, 129.42, 129.02, 126.75, 21.35 (d, J_{CP} = 23 Hz) ppm. ^{31}P NMR (C_6D_6): δ_P −28.54 ppm. IR: 3054, 2963, 2908, 2824, 1693, 1584, 1449, 1391, 1290, 1261, 1199, 1116, 1034, 843, 823, 800, 746, 716, 556, 528, 507, 481 cm^{-1}.

*P^{Ph}CNP^{oTol} (**4**).* The whole procedure was performed under inert conditions and with dry and degassed solvents. 2-Di-*o*-tolyl-phosphanyl-benzaldehyde (4.00 g, 0.013 mol), 2-diphenylphosphinoaniline (3.48 g, 0.013 mol), and *p*-toluene sulfonic acid (60 mg, 0.32 mmol) were dissolved in toluene (110 mL) in a 3-necked round-bottom flask under an N_2 atmosphere. A Dean−Stark trap was attached, and the tap was filled with molecular sieves (3 Å). The clear yellow-brown solution was heated to reflux for 17 h, and the color changed to red/yellow-brown, after which all solvents were evaporated. CH_2Cl_2 was added (20 mL), subsequently MeOH was added (20 mL), and the mixture was cooled in an ice bath for 20 min to precipitate the crude product. The solids were washed with MeOH until the supernatant was colorless, and the solids were dried in vacuum resulting in **4** as a yellow powder with a yield of 47% (3.43 g, 5.94 mmol). ^{1}H NMR (C_6D_6): δ_H 9.33 (d, J = 6 Hz, 1H, −N═C*H*−), 8.43 (ddd, J = 8, 4, 1 Hz, 1H, Ar−*H*), 7.46−7.42 (m, 4H, Ar−*H*), 7.06−6.93 (m, 16H, Ar−*H*), 6.87−6.80 (m, 4H, Ar−*H*), 6.59 (ddd, J = 8, 4, 1 Hz, 1H, Ar−*H*), 2.34 (s, 6H, −C*H*$_3$) ppm. ^{13}C NMR (C_6D_6): δ_C 158.08 (dd, J_{CP} = 2, 28 Hz), 155.13 (d, J_{CP} = 18 Hz),

DOI: 10.1021/acs.inorgchem.8b01478
Inorg. Chem. 2018, 57, 10846−10856

142.76 (d, J_{CP} = 25 Hz), 140.49 (d, J_{CP} = 17 Hz), 138.14 (d, J_{CP} = 12 Hz), 137.21 (d, J_{CP} = 19 Hz), 134.79, 134.61 (d, J_{CP} = 21 Hz), 133.95, 133.74, 133.59 (d, J_{CP} = 13 Hz), 133.10, 131.34, 130.59 (d, J_{CP} = 4 Hz), 130.09, 129.39, 129.33, 128.68, 128.60, 128.41 (d, J_{CP} = 4 Hz), 126.84, 126.25, 117.47 (d, J_{CP} = 2 Hz), 21.39 (d, J_{CP} = 22 Hz) ppm. ^{31}P NMR (C_6D_6): δ_P −13.49, −31.62 ppm. IR: 3048, 3004, 2965, 2941, 2912, 2875, 1698, 1627, 1618, 1561, 1466, 1431, 1357, 1265, 1191, 1118, 1093, 1068, 1024, 861, 766, 747, 740, 695, 555, 503, 457 cm^{-1}. ESI-MS (MeCN/formic acid) *m/z*: calcd: 578.2167, found: 578.2456. Elemental analysis: calcd: C 81.09, H 5.76, N 2.42; found: C 80.68, H 5.89, N 2.41.

*$P^{oTol}CNP^{oTol}$ (**5**).* The same method was used as for **4** with adjusted amounts: 2-di-*o*-tolyl-phosphanyl-benzaldehyde (0.258 g, 0.810 mmol), 2-di-*o*-tolyl-phosphinoaniline (0.252 g, 0.825 mmol), *p*-toluene sulfonic acid (8 mg, 0.042 mmol), and toluene (20 mL). After the procedure **5** was obtained as an off-white/yellow powder with a yield of 82% (0.400 g, 0.66 mmol). ^{1}H NMR (C_6D_6): δ_H 9.32 (d, *J* = 6 Hz, 1H, −N═C*H*−), 8.38 (m, 1H, Ar−*H*), 6.79−7.10 (m, 22H, Ar−*H*), 6.59 (dd, *J* = 3, 5 Hz, 1H, Ar−*H*), 2.51 (s, 6H, −CH_3), 2.33 (s, 6H, −CH_3) ppm. ^{13}C NMR (C_6D_6): δ_C 158.12 (dd, J_{CP} = 2, 27 Hz), 155.72 (d, J_{CP} = 19 Hz), 142.92 (d, J_{CP} = 26 Hz), 142.79 (d, J_{CP} = 27 Hz), 140.59 (d, J_{CP} = 18 Hz), 137.35 (d, J_{CP} = 18 Hz), 135.96 (d, J_{CP} = 13 Hz), 134.79 (d, J_{CP} = 10 Hz), 134.15, 133.96, 133.52 (d, J_{CP} = 46 Hz), 131.63 (d, J_{CP} = 12 Hz), 131.28, 130.58 (d, J_{CP} = 4.6 Hz), 130.29 (d, J_{CP} = 4.4 Hz), 130.16, 129.30 (d, J_{CP} = 6 Hz), 129.31, 128.81, 128.35, 126.82, 126.47, 126.31, 125.70, 21.61−21.28 (21.61, 21.49, 21.38, 21.28:4 signals, 2*d*, assignment unknown) ppm. ^{31}P NMR (C_6D_6): δ_P −30.28, −31.56 ppm. IR: 3057, 2967, 2934, 2864, 1625, 1586, 1564, 1464, 1380, 1356, 1264, 1129, 1033, 800, 750, 733, 717, 555, 485, 453 cm^{-1}. ESI-MS (MeCN/formic acid) *m/z*: [M]$^+$ calcd: 606.2479, found: 606.2273. Elemental analysis: calcd: C 81.30, H 6.16, N 2.31; found: C 80.91, H 6.36, N 2.17.

*$Ni(P^{Ph}CNP^{oTol})(PPh_3)$ (**6**).* $P^{Ph}CNP^{oTol}$ (**4**) (252.4 mg, 0.437 mmol), PPh_3 (115.8 mg, 0.441 mmol), and $Ni(cod)_2$ (120.5 mg, 0.438 mmol) were combined in a vial, and THF (5 mL) was added, resulting in a red/brown solution. The mixture was stirred overnight, after which the mixture was concentrated to ∼2 mL. Hexanes (6 mL) were added, and the vial was placed at −35 °C for 1 h. The solids were isolated by filtration and redissolved in toluene. After evaporation of all solvents, **6** was obtained with a yield of 90% (352.1 mg, 0.392 mmol). Single crystals for XRD analysis were grown by slow vapor diffusion of hexanes into THF. ^{1}H NMR (C_6D_6): δ_H 7.77 (t, *J* = 9 Hz, 2H, Ar−*H*), 7.40 (s, broad, Ar−*H*), 7.30 (t, *J* = 6 Hz, Ar−*H*), 7.24 (m, Ar−*H*), 7.13−6.86 (m, Ar−*H*), 6.79−6.68 (m, Ar−*H*), 5.88 (t, *J* = 7 Hz, 1H, Ar−*H*), 2.54 (s, 3H, *o*Tol−Me), 1.88 (s, 3H, *o*Tol−Me) ppm. ^{13}C NMR (C_6D_6): δ_C 166.83 (dd, J_{CP} = 4, 28 Hz), 153.86 (d, J_{CP} = 33 Hz), 142.06, 141.95, 138.41, 138.15, 137.87, 137.52, 137.28, 136.24, 136.09, 135.50, 133.97 (d, J_{CP} = 13 Hz), 133.50 (d, J_{CP} = 14 Hz), 132.95, 132.95 (d, J_{CP} = 11 Hz), 131.83 (m), 131.49 (d, J_{CP} = 4 Hz), 130.16, 129.34, 126.24, 126.03 (dd, J_{CP} = 4, 11 Hz), 125.74 (m), 125.15 (d, J_{CP} = 4 Hz), 120.27 (d, J_{CP} = 5 Hz), 119.11 (broad), 22.98, 22.91 ppm. ^{31}P NMR (C_6D_6): δ_P 36.02, 28.79, 1.09 ppm. IR: 3047, 1585, 1570, 1453, 1433, 1387, 1297, 1089, 1026, 818, 740, 693, 514, 484, 460, 407 cm^{-1}. Crystals for X-ray analysis were grown from THF/hexanes. Elemental analysis: calcd: C 76.19, H 5.38, N 1.56; found: C 75.99, H 5.57, N 1.46.

*$Ni(P^{oTol}CNP^{oTol})(PPh_3)$ (**7**).* $P^{oTol}CNP^{oTol}$ (**5**) (40.0 mg, 0.066 mmol), PPh_3 (17.3 mg, 0.066 mmol), and $Ni(cod)_2$ (18.2 mg, 0.066 mmol) were combined in a vial, and THF (5 mL) was added, resulting in a red/brown solution. The mixture was stirred overnight, after which the mixture was concentrated to ∼1.5 mL. Hexanes (8 mL) was added, and the vial was placed at −35 °C for 2 h. The solids were isolated by filtration, washed with hexanes (3 × 2 mL), and collected by dissolution in toluene. After evaporation of all solvents, **7** was obtained with a yield of 94% (57.5 mg, 0.062 mmol). Single crystals for XRD analysis were grown by slow vapor diffusion of hexanes into THF. ^{1}H NMR (C_6D_6): δ_H 7.73 (broad singlet, 2H, Ar−*H*), 7.41 (broad singlet, 6H, Ar−*H*), 7.20 (broad singlet, 1H, Ar−*H*), 7.12−6.72 (m, 30H, Ar−*H*), 6.45 (t, *J* = 7 Hz, 1H, imine−C*H* (or Ar−*H*)), 6.17 (broad singlet, 1H, Ar−*H* (or imine−C*H*)), 5.81 (dd, *J* = 3, 8 Hz, 1H, Ar−*H* (or imine−C*H*)), 2.48 (broad singlet, 6H, *o*Tol−Me) 2.43 (broad singlet, 3H, *o*Tol−Me), 1.76 (broad singlet, 3H, *o*Tol−Me) ppm. ^{13}C NMR (C_6D_6): δ_C 165.23 (broad), 149.68 (broad), 143.10, 142,71, 141.82, 135.86, 135.49, 134.19 (d, J_{CP} = 14 Hz), 133.87, 133.40, 132.98, 131.91, 131.28, 130.79, 130.34, 130.05, 129.11, 128.69, 126.68, 126.35, 126.04, 125.93, 123.47, 120.16, 117.71, 23.07, 21.70, 21.48, 21.12 ppm. ^{31}P NMR (C_6D_6): δ_P 39.90, 10.80, − 27.72 ppm. IR: 3052, 2969, 2924, 2854, 1952, 1919, 1811, 1669, 1573, 1454, 1435, 1392, 1309, 1260, 1202, 1159, 1118, 1093, 1026, 803, 748, 716, 695, 572, 521, 487, 460 cm^{-1}. Crystals for X-ray analysis were grown from THF/hexanes. The compound is too sensitive for transportation for elemental analysis.

*$[Ni(P^{Ph}CNP^{Ph})]_2$ (**8**).* $P^{Ph}CNP^{Ph}$ (**1**) (150.2 mg, 0.273 mmol) was suspended in toluene (2 mL). In a second vial, $Ni(COD)_2$ (74.9 mg, 0.272 mmol) was suspended in toluene (6 mL) and transferred to the ligand suspension. The yellow suspension directly changed color to a turbid yellow-brown mixture and was left to stir for 5 h. All solvent was evaporated, and the remaining solids were dissolved in THF (1 mL). The product was precipitated by addition of 8 mL of hexanes, followed by cooling the mixture to −35 °C before the solids were collected by filtration. The solids were collected by dissolution in THF, after which the solvents were evaporated. The mixture was dried under vacuum for 2 nights, after which the product mixture was obtained with a yield of 96% (159.6 mg, 0.131 mol). ^{1}H NMR (C_6D_6) major species **8a**: δ_H 7.83−7.78 (m, Ar−*H*), 7.66−7.61 (m, Ar−*H*), 7.58−7.53 (m, Ar−*H*), 7.47 (ddd, *J* = 1, 3, 5 Hz, Ar−*H*), 7.35−7.30 (m, Ar−*H*), 7.25 (dt, *J* = 2, 8 Hz, Ar−*H*), 7.13−6.44 (m, Ar−*H*), 6.39−6.35 (m, 1H, Ar−*H*), 5.49 (d, *J* = 2 Hz, 1H, C*H*−CH or imine−C*H*), 4.58, (d, *J* = 6 Hz, 1H, CH−C*H* or imine−C*H*) ppm. Minor species **8b**: δ_H 7.91 (t, *J* = 8 Hz, Ar−*H*), 7.21 (s, Ar−*H*), 7.19 (s, Ar−*H*), 6.29 (t, *J* = 8 Hz, Ar−*H*), 6.17 (t, *J* = 7 Hz, Ar−*H*), 5.31 (m), 3.88 (s) ppm. ^{13}C NMR (C_6D_6) **8a** + **8b**: δ_C 166.28 (d, J_{CP} = 38 Hz), 152.39 (d, J_{CP} = 38 Hz), 151.91 (dd, J_{CP} = 5, 15 Hz), 143.64 (d, J_{CP} = 12 Hz), 143.16 (d, J_{CP} = 11 Hz), 140.95, 140.66 (d, J_{CP} = 10 Hz), 140.43, 140.16, 139.92, 139.12, 139.04, 138.78, 138.601 (d, J_{CP} = 7 Hz), 140.65 (d, J_{CP} = 10 Hz), 139.13, 139.04, 138.78, 137.61 (d, J_{CP} = 7 Hz), 136.78 (d, J_{CP} = 5 Hz), 136.42, 136.16, 135.72, 135.56, 135.08, 134.93, 133.70, 133.61, 133.52, 133.46, 133.39, 133.26, 133.11, 133.01, 132.88, 132.73, 132.63, 132.21, 132.09, 131.56, 130.72, 130.06, 129.39, 129.34, 129.27, 129.13, 128.91, 128.82, 128.69, 128.57, 128.50, 127.53, 127.33, 125.70, 123.54, 121.24, 120.39, 117.32, 87.24 (d, J_{CP} = 26 Hz), 79.13 (d, J_{CP} = 6 Hz). ^{31}P NMR (C_6D_6) 8a: δ_P 35.5 (dd, J_{PP} = 2, 70 Hz), 35.4 (d, J_{PP} = 9 Hz), 22.9 (dd, J_{PP} = 2, 9 Hz), − 7.9 (d, J_{PP} = 70 Hz); 8b: 38.32 (d, J_{PP} = 43 Hz), 1.05 (d, J_{PP} = 43 Hz) ppm. IR: 3048, 2856, 1580, 1568, 1477, 1449, 1431, 1325, 1251, 1202, 1090, 1065, 1026, 919, 850, 735, 693, 497 cm^{-1}.

*$[Ni(P^{Ph}CNP^{Ph})]_2(CO)_2$ (**9a** and **9b**).* **8** (8.4 mg, 6.9 μmol, the obtained mixture of **8a** and **8b** was used) was dissolved in C_6D_6 (0.6 mL) and transferred to a Young-type NMR tube. The mixture was degassed to remove the N_2 atmosphere (2 freeze−pump−thaw cycles) and charged with CO (1 atm) upon thawing of the solution. The tube was regularly shaken, and the color of the mixture changed overnight from turbid red to clear orange. The progress of the reaction was monitored by NMR analysis (see Supporting Information, Figure S42). The NMR tube was placed back in the glovebox, after which the mixture was filtered and transferred to a small reaction tube. The reaction tube was placed in a vial, and hexanes (1 mL) was placed in the vial (crystallization setup) for crystallization to take place. After 2 days, crystals were formed, and the liquid phase was removed by decantation. The crystals were washed with hexanes (3 × 1.5 mL) and dried in vacuum for no longer than 5 min, resulting in **9b**. The liquid phase was dried in vacuum as well, resulting in the bulk material **9a**.

9b: **9b** was isolated as red-brown crystals with a yield of 21% (1.8 mg, 1.4 μmol). ^{1}H NMR (C_6D_6): δ_H 10.10 (dd, *J* = 4, 8 Hz, 2H, Ar−*H*), 7.91 (t, *J* = 2, 8 Hz, 4H, Ar−*H*), 7.75 (t, *J* = 8 Hz, 4H, Ar−*H*), 7.47 (m, 6H, Ar−*H*), 7.31 (m, 4H, Ar−*H*), 7.12−6.86 (m, 20H, Ar−*H*), 6.79−6.66 (m, 10H, Ar−*H*), 6.58 (t, *J* = 8 Hz, 2H, Ar−*H*), 6.50 (s, broad, 2H, Ar−*H*), 6.18 (t, *J* = 7 Hz, 2H, C*H*−C*H*), 5.95 (d,

DOI: 10.1021/acs.inorgchem.8b01478
Inorg. Chem. 2018, 57, 10846−10856

broad, J = 9 Hz, 2H, Ar−*H*) ppm. ^{13}C NMR (C_6D_6): δ_C 198.24 (−CO), 150.97, 134.75, 134.69, 134.62, 133.65, 133.59, 133.21, 133.12, 133.07, 132.70, 132.14, 132.07, 131.61, 130.09, 129.96, 129.51, 128.69, 126.53, 113.81, 112.79, 70.35 ppm. ^{31}P NMR (C_6D_6): δ_P 39.81, 22.12 ppm. IR: 3051, 2963, 2922, 2853, 1999, 1938, 1680 (broad), 1578, 1479, 1452, 1435, 1328, 1260, 1095, 1026, 799, 740, 692, 526, 511, 499, 456 cm^{-1}.

9a (bulk): **9a** was not isolated and only observed as a mixture together with an unknown byproduct. The mixture is a brown solid. Major signals in ^{1}H NMR (C_6D_6): δ_H 8.03 (t, *J* = 3 Hz, Ar−*H*), 7.84 (d, *J* = 2 Hz, Ar−*H* or N═C*H*), 7.62−7.52 (m, Ar−*H*), 7.22 (t, *J* = 8 Hz, Ar−*H*), 7.12 (dt, *J* = 1, 7 Hz, Ar−*H*), 7.01 (d, *J* = 1 Hz, Ar−*H*), 7.00−6.98 (m, Ar−*H*), 6.94−6.89 (m, Ar−*H*), 6.87 (t, *J* = 1 Hz, Ar−*H*), 6.85 (t, *J* = 1 Hz, Ar−*H*), 6.76 (t, *J* = 8 Hz, Ar−*H*), 6.27 (ddd, *J* = 1, 3, 5 Hz, Ar−*H*) ppm. Major signals in ^{13}C NMR (C_6D_6): δ_C 200.24 (dd, J_{CP} = 5, 6 Hz, − CO), 156.55, 154.58, 154.43, 139.36 (d, J_{CP} = 4 Hz), 139.04 (d, J_{CP} = 4 Hz), 138.95 (d, J_{CP} = 6 Hz), 138.78 (d, J_{CP} = 1 Hz), 138.66 (d, J_{CP} = 6 Hz), 138.08 (d, J_{CP} = 7 Hz), 134.93 (d, J_{CP} = 3 Hz), 133.96, 133.76, 133.62, 133.46, 133.33, 133.27 (d, J_{CP} = 5 Hz), 130.98, 130.32 (d, J_{CP} = 6 Hz), 129.33, 128.92 (d, J_{CP} = 1 Hz), 128.68, 128.58 (d, J_{CP} = 1 Hz), 128.50, 128.42, 128.36, 127.40, 127.06, 126.80, 15.85 (d, J_{CP} = 4 Hz), 125.70, 117.76 (d, J_{CP} = 5 Hz), 110.42 ppm. ^{31}P NMR (C_6D_6): δ_P 33.04 (d, J_{PP} = 11 Hz), 16.23 (d, J_{PP} = 11 Hz) ppm. Unidentified impurity: δ_P 26.32 (d, *J* = 25 Hz), 23.08 (d, *J* = 25 Hz) ppm. Major signals in IR: 3054, 3002, 2957, 2925, 2855, 2068, 1991, 1929, 1629, 1578, 1460, 1434, 1266, 1184, 1090, 1028, 884, 766, 744, 695, 508 cm^{-1}.

■ ASSOCIATED CONTENT

Supporting Information

The Supporting Information is available free of charge on the ACS Publications website at DOI: 10.1021/acs.inorgchem.8b01478.

Spectroscopic data (PDF)

Accession Codes

CCDC 1845433−1845438 contain the supplementary crystallographic data for this paper. These data can be obtained free of charge via www.ccdc.cam.ac.uk/data_request/cif, or by emailing data_request@ccdc.cam.ac.uk, or by contacting The Cambridge Crystallographic Data Centre, 12 Union Road, Cambridge CB2 1EZ, UK; fax: +44 1223 336033.

■ AUTHOR INFORMATION

Corresponding Author

*E-mail: M.Moret@uu.nl.

ORCID

Marc-Etienne Moret: 0000-0002-3137-6073

Notes

The authors declare no competing financial interest.

■ ACKNOWLEDGMENTS

We thank the Sectorplan Natuur-en Scheikunde (Tenure-track grant at Utrecht University) and The Netherlands Organization for Scientific Research (NWO, ECHO-STIP grant) for financial support. Support with NMR spectroscopic analysis by Dr. J. T. B. H. Jastrzebski is gratefully acknowledged. The X-ray diffractometer was financed by NWO. This work was sponsored by NWO Exacte en Natuurwetenschappen (Physical Sciences) for the use of supercomputer facilities, with financial support from The Netherlands Organization for Scientific Research (NWO). The DFT work was carried out on the Dutch national e-infrastructure with the support of the SURF Foundation.

■ REFERENCES

(1) Khusnutdinova, J. R.; Milstein, D. Metal−Ligand Cooperation. *Angew. Chem., Int. Ed.* **2015**, *54*, 12236−12273.

(2) Chirik, P. J.; Wieghardt, K. Radical Ligands Confer Nobility on Base-Metal Catalysts. *Science* **2010**, *327*, 794−795.

(3) Verhoeven, D. G. A.; Moret, M.-E. Metal−ligand cooperation at tethered π-ligands. *Dalton Trans.* **2016**, *45*, 15762−15778.

(4) van der Vlugt, J. I. Cooperative Catalysis with First-Row Late Transition Metals. *Eur. J. Inorg. Chem.* **2012**, *2012*, 363−375.

(5) (a) Bennett, M. A.; Clark, P. W. Tridentate chelate π-bonded complexes of rhodium(I), iridium(I), and iridium(III) and chelate σ-bonded complexes of nickel(II), palladium(II), and platinum(II) formed by intramolecular hydrogen abstraction reactions. *J. Organomet. Chem.* **1976**, *110* (3), 367−381. (b) Bennett, M. A.; Johnson, R. N.; Tomkins, I. B. Additions to metal atom and to coordinated ligand in complexes of rhodium(I) and iridium(I) formed by a tridentate olefinic ditertiary phosphine: chelate olefin complexes and σ-alkyls of rhodium(III) and iridium(III). *J. Organomet. Chem.* **1976**, *118*, 205−232. (c) Barrett, B. J.; Iluc, V. M. Group 10 Metal Complexes Supported by Pincer Ligands with an Olefinic Backbone. *Organometallics* **2014**, *33*, 2565−2574. (d) Barrett, B. J.; Iluc, V. M. Coordination of a Hemilabile Pincer Ligand with an Olefinic Backbone to Mid-to-Late Transition Metals. *Inorg. Chem.* **2014**, *53*, 7248−7259. (e) Comanescu, C. C.; Vyushkova, M.; Iluc, V. M. Palladium carbene complexes as persistent radicals. *Chem. Sci.* **2015**, *6*, 4570−4579. (f) Campos, J.; Ortega-Moreno, L.; Conejero, S.; Peloso, R.; Lopez-Serrano, J.; Maya, C.; Carmona, E. *Chem. - Eur. J.* **2015**, *21*, 8883−8896.

(6) Saes, B. W. H.; Verhoeven, D. G. A.; Lutz, M.; Klein Gebbink, R. J. M.; Moret, M.-E. Coordination of a Diphosphine−Ketone Ligand to Ni(0), Ni(I), and Ni(II): Reduction-Induced Coordination. *Organometallics* **2015**, *34*, 2710−2713.

(7) Verhoeven, D. G. A.; van Wiggen, M. A. C.; Kwakernaak, J.; Lutz, M.; Klein Gebbink, R. J. M.; Moret, M.-E. Periodic Trends in the Binding of a Phosphine-Tethered Ketone Ligand to Fe, Co, Ni, and Cu. *Chem. - Eur. J.* **2018**, *24*, 5163.

(8) Fache, F.; Schulz, E.; Tommasino, M. L.; Lemaire, M. Nitrogen-Containing Ligands for Asymmetric Homogeneous and Heterogeneous Catalysis. *Chem. Rev.* **2000**, *100*, 2159−2231.

(9) Examples are: Salen ligand: (a) Canali, L.; Sherrington, D. C. Utilisation of homogeneous and supported chiral metal(salen) complexes in asymmetric catalysis. *Chem. Soc. Rev.* **1999**, *28*, 85−93. (b) Kleij, A. W. Nonsymmetrical Salen Ligands and Their Complexes: Synthesis and Applications. *Eur. J. Inorg. Chem.* **2009**, *2009*, 193−205. Morris complexes: (c) Sues, P. E.; Demmans, K. Z.; Morris, R. H. Rational development of iron catalysts for asymmetric transfer hydrogenation. *Dalton Trans.* **2014**, *43*, 7650−7667. (d) Smith, S. A. M.; Lagaditis, P. O.; Lupke, A.; Lough, A. J.; Morris, R. H. Unsymmetrical Iron P-NH-P′ Catalysts for the Asymmetric Pressure Hydrogenation of Aryl Ketones. *Chem. - Eur. J.* **2017**, *23*, 7212−7216. Noyori complex: (e) Gao, J.-X.; Ikariya, T.; Noyori, R. A Ruthenium(II) Complex with a C_2-Symmetric Diphosphine/Diamine Tetradentate Ligand for Asymmetric Transfer Hydrogenation of Aromatic Ketones. *Organometallics* **1996**, *15*, 1087−1089. Iminopyrrole ligands: (f) Han, F.-B.; Zhang, Y.-L.; Sun, X.-L.; Li, B.-G.; Guo, Y.-H.; Tang, Y. Synthesis and Characterization of Pyrrole-imine [N−NP] Nickel(II) and Palladium(II) Complexes and Their Applications to Norbornene Polymerization. *Organometallics* **2008**, *27*, 1924−1928. Pyridine-Imine ligands: (g) Chen, Z.; Allen, K. E.; White, P. S.; Daugulis, O.; Brookhart, M. Synthesis of Branched Polyethylene with "Half-Sandwich" Pyridine-Imine Nickel Complexes. *Organometallics* **2016**, *35*, 1756−1760. (h) Zhu, D.; Thapa, I.; Korobkov, I.; Gambarotta, S.; Budzelaar, P. H. M. Redox-Active Ligands and Organic Radical Chemistry. *Inorg. Chem.* **2011**, *50* (20), 9879−9887. (i) Volpe, E. C.; Wolczanski, P. T.; Lobkovsky, E. B. Aryl-Containing Pyridine-Imine and Azaallyl Chelates of Iron toward Strong Field Coordination Compounds. *Organometallics* **2010**, *29*, 364−377. Dinuclear Ni-complexes: (j) Steiman, T. J.; Uyeda, C. Reversible Substrate Activation and

DOI: 10.1021/acs.inorgchem.8b01478
Inorg. Chem. 2018, 57, 10846−10856

Catalysis at an Intact Metal−Metal Bond Using a Redox-Active Supporting Ligand. *J. Am. Chem. Soc.* **2015**, *137* (18), 6104−6110.
(10) Britovsek, G. J. P.; Gibson, V. C.; McTavish, S. J.; Solan, G. A.; White, A. J. P.; Williams, D. J.; Kimberley, B. S.; Maddox, P. J. Novel olefin polymerization catalysts based on iron and cobalt. *Chem. Commun.* **1998**, *7*, 849−850.
(11) Small, B. L.; Brookhart, M.; Bennett, A. M. A. Highly Active Iron and Cobalt Catalysts for the Polymerization of Ethylene. *J. Am. Chem. Soc.* **1998**, *120* (16), 4049−4050.
(12) Chirik, P. J. Carbon−Carbon Bond Formation in a Weak Ligand Field: Leveraging Open-Shell First-Row Transition-Metal Catalysts. *Angew. Chem., Int. Ed.* **2017**, *56* (19), 5170−5181.
(13) Hou, J.; Sun, W.-H.; Zhang, S.; Ma, H.; Deng, Y.; Lu, X. Synthesis and Characterization of Tridentate Nickel Complexes Bearing P∧N∧N and P∧N∧P Ligands and Their Catalytic Property in Ethylene Oligomerization. *Organometallics* **2006**, *25* (1), 236−244.
(14) Chen, L.; Ai, P.; Gu, J.; Jie, S.; Li, B.-G. Stereospecific polymerization of 1,3-butadiene catalyzed by cobalt complexes bearing *N*-containing diphosphine PNP ligands. *J. Organomet. Chem.* **2012**, *716*, 55−61.
(15) Doherty, S.; Knight, J. G.; Scanlan, T. H.; Elsegood, M. R. J.; Clegg, W. Iminophosphines: synthesis, formation of 2,3-dihydro-1*H*-benzo[1,3]azaphosphol-3-ium salts and *N*-(pyridin-2-yl)-2-diphenylphosphinoylaniline, coordination chemistry and applications in platinum group catalyzed Suzuki coupling reactions and hydrosilylations. *J. Organomet. Chem.* **2002**, *650*, 231−248.
(16) Crociani, B.; Antonaroli, S.; Paoli, P.; Rossi, P. η^1-Allylpalladium complexes with a tridentate PNP ligand with different phosphino groups. *Dalton Trans.* **2012**, *41*, 12490−12500.
(17) (a) Hoberg, H.; Gotz, V.; Kruger, C.; Tsay, Y.-H. Darstellung, Eigenschaften und bindungsverhältnisse von benzophenoniminonickel(0)-komplexen. *J. Organomet. Chem.* **1979**, *169*, 209−217. (b) Manan, R. S.; Kilaru, P.; Zhao, P. Nickel-Catalyzed Hydroimination of Alkynes. *J. Am. Chem. Soc.* **2015**, *137* (19), 6136−6139. (c) Hoshimoto, Y.; Ohata, T.; Ohashi, M.; Ogoshi, S. Nickel-catalyzed synthesis of N-aryl-1,2-dihydropyridines by [2 + 2+2] cycloaddition of imines with alkynes through T-shaped 14-electron aza-nickelacycle key intermediates. *Chem. - Eur. J.* **2014**, *20* (14), 4105−4110. (d) Iglesias, A. L.; Muñoz-Hernández, M.; García, J. J. Fluoro aromatic imine nickel(0) complexes: Synthesis and structural studies. *J. Organomet. Chem.* **2007**, *692* (16), 3498−3507. (e) Cámpora, J.; Matas, I.; Palma, P.; Álvarez, E.; Graiff, C.; Tiripicchio, A. Monomeric Alkoxo and Amido Methylnickel(II) Complexes. Synthesis and Heterocumulene Insertion Chemistry. *Organometallics* **2007**, *26* (15), 3840−3849. (f) Weng, Z.; Teo, S.; Koh, L. L.; Hor, T. S. A. Ethylene Oligomerization at Coordinatively and Electronically Unsaturated Low-Valent Nickel. *Angew. Chem., Int. Ed.* **2005**, *44* (46), 7560−7564.
(18) Reed, B. R.; Yousif, M.; Lord, R. L.; McKinnon, M.; Rochford, J.; Groysman, S. Coordination Chemistry and Reactivity of Bis(aldimino)pyridine Nickel Complexes in Four Different Oxidation States. *Organometallics* **2017**, *36*, 582−593.
(19) Tejel, C.; Ciriano, M. A.; Pilar del Rio, M.; van den Bruele, F. J.; Hetterscheid, D. G. H.; Tsichlis i Spithas, N.; de Bruin, B. Deprotonation Induced Ligand-to-Metal Electron Transfer: Synthesis of a Mixed-Valence Rh(−I,I) Dinuclear Compound and Its Reaction with Dioxygen. *J. Am. Chem. Soc.* **2008**, *130*, 5844−5845.
(20) Maire, P.; Sreekanth, A.; Büttner, T.; Harmer, J.; Gromov, I.; Rüegger, H.; Breher, F.; Schweiger, A.; Grützmacher, H. Synthesis of a Rhodaazacyclopropane and Characterization of Its Radical Cation by EPR Spectroscopy. *Angew. Chem., Int. Ed.* **2006**, *45*, 3265−3269.
(21) Dzik, W. I.; Calvo, S. E.; Reek, J. N. H.; Lutz, M.; Ciriano, M. A.; Tejel, C.; Hetterscheid, D. G. H.; de Bruin, B. Binuclear $[(cod)(Cl)Ir(bpi)Ir(cod)]^+$ for Catalytic Water Oxidation. *Organometallics* **2011**, *30*, 372−374.
(22) Tejel, C.; Asensio, L.; del Río, M. P.; de Bruin, B.; López, J. A.; Ciriano, M. A. Snapshots of a Reversible Metal-Ligand Two-Electron Transfer Step Involving Compounds Related by Multiple Types of Isomerism. *Eur. J. Inorg. Chem.* **2012**, *2012*, 512−519.
(23) Tejel, C.; Asensio, L.; del Río, M. P.; de Bruin, B.; López, J. A.; Ciriano, M. A. Developing Synthetic Approaches with Non-Innocent Metalloligands: Easy Access to Ir^I/Pd^0 and $Ir^I/Pd^0/Ir^I$ Cores. *Angew. Chem., Int. Ed.* **2011**, *50*, 8839−8843.
(24) Büttner, T.; Breher, F.; Grützmacher, H. Amine olefin rhodium(I) complexes: pK_a and NH bond strength. *Chem. Commun.* **2004**, 2820−2821.
(25) Ainscough, E. W.; Brodie, A. M.; Buckley, P. D.; Burrell, A. K.; Kennedy, S. M. F.; Waters, J. M. Synthesis, structure and kinetics of Group 6 metal carbonyl complexes containing a new 'P_2N' mixed donor multidentate ligand. *Dalton. Trans.* **2000**, 2663.
(26) The signal likely shifts to a more crowded region and could not be assigned unambiguously.
(27) A related complex based on Pt has been reported: Ainscough, E. W.; Brodie, A. M.; Burrell, A. K.; Derwahl, A.; Jameson, G. B.; Taylor, S. K. Platinum(II) and palladium(II) complexes containing a mixed donor`P_2N' multidentate ligand. *Polyhedron* **2004**, *23*, 1159−1168.
(28) Similar experiments with more bulky ligands **4** and **5** lead to unassigned mixtures of products.
(29) Chu, W.-Y.; Gilbert-Wilson, R.; Rauchfuss, T. B.; van Gastel, M.; Neese, F. Cobalt Phosphino-α-Iminopyridine-Catalyzed Hydrofunctionalization of Alkenes: Catalyst Development and Mechanistic Analysis. *Organometallics* **2016**, *35* (17), 2900−2914.
(30) A COSY spectrum shows no coupling of these signals. The peaks do not appear as doublets, so if a coupling would be present it would be small. In a C−C bound structure, these protons would be located in vicinal positions. In complex 9 this vicinal angle is determined around 75−80° (determined in XRD of calculated positions and in geom opt structure by DFT), which leads to a very small coupling (0−2 Hz based on the Karplus curve), and so it is likely this is not observed. *Spectroscopic Methods in Organic Chemistry*; Hesse, M.; Meier, H.; Zeeh, B. Georg Thieme Verslag: Stuttgart, 2008; p 113.
(31) Chu, W.-Y.; Richers, C. P.; Kahle, E. R.; Rauchfuss, T. B. Imine-Centered Reactions in Imino-Phosphine Complexes of Iron Carbonyls. *Organometallics* **2016**, *35*, 2782−2792.
(32) Lei, H.; Royer, A. M.; Rauchfuss, T. B.; Gray, D. C_2-Symmetric Iron(II) Diphosphine−Dialkoxide Dicarbonyl and Related Complexes. *Organometallics* **2012**, *31* (17), 6408−6414.
(33) Other imine couplings: (a) Floriani, C.; Solari, E.; Franceschi, F.; Scopelliti, R.; Belanzoni, P.; Rosi, M. Metal-metal and carbon-carbon bonds as potential components of molecular batteries. *Chem. - Eur. J.* **2001**, *7* (14), 3052−3061. (b) Franceschi, F.; Solari, E.; Scopelliti, R.; Floriani, C. Metal-Mediated Transfer of Electrons between Two Different C−C Single Bonds That Function as Electron-Donor and Electron-Acceptor Units. *Angew. Chem., Int. Ed.* **2000**, *39* (9), 1685−1987. (c) de Angelis, S.; Solari, E.; Gallo, E.; Floriani, C.; Chiesi-Villa, A.; Rizzoli, C. Formation of Carbon-Carbon-Bonded Dimers in the Reduction of [Co^{II}salophen] [salophen = *N,N′-o*-Phenylenebis(salicylideneaminato)]: Their Reactivity with Electrophiles To Form Co−C Bonds. *Inorg. Chem.* **1996**, *35*, 5995−6003. (d) Andrez, J.; Guidal, V.; Scopelliti, R.; Pécaut, J.; Gambarelli, S.; Mazzanti, M. *J. Am. Chem. Soc.* **2017**, *139*, 6828−6838.
(34) Cooper, M. K.; Duckworth, P. A.; Hambley, T. W.; Organ, G. J.; Henrick, K.; McPartlin, M.; Parekh, A. Synthesis of a new P_2N_2 ligand *N,N′*-bis[2-(diphenylphosphino)phenyl]propane-1,3-diamine, H_2L^2, and some of its complexes with elements of the nickel triad and rhodium: *X*-ray structure analyses of the neutral complex $[NiL^2]$ and the trans-spanned $[Rh(CO)Cl(H_2L^2)]$. *J. Chem. Soc., Dalton Trans.* **1989**, *6*, 1067−1073.
(35) Other pinacol couplings: (a) Folkertsma, E.; Benthem, S. H.; Witteman, L.; van Slagmaat, C. A. M. R.; Lutz, M.; Klein Gebbink, R. J. M.; Moret, M.-E. Formation of exceptionally weak C−C bonds by metal-templated pinacol coupling. *Dalton Trans.* **2017**, *46* (19), 6177−6182. (b) Hou, Z.; Fujita, A.; Zhang, Y.; Miyano, T.; Yamazaki, H.; Wakatsuki, Y. One-Electron Reduction of Aromatic Ketones by Low-Valent Lanthanides. Isolation, Structural Characterization, and

DOI: 10.1021/acs.inorgchem.8b01478
Inorg. Chem. 2018, 57, 10846−10856

Reactivity of Lanthanide Ketyl Complexes. *J. Am. Chem. Soc.* **1998**, *120*, 754−766.

(36) (a) Nicolas, E.; Ohleier, A.; D'Accriscio, F.; Põcharman, A.-F.; Demange, M.; Ribagnac, P.; Ballester, J.; Gosmini, C.; Mõzailles, N. "(Diphosphine)Nickel"-catalyzed negishi cross-coupling: an experimental and theoretical study. *Chem. - Eur. J.* **2015**, *21*, 7690−7694. (b) Desnoyer, A. N.; Bowes, E. G.; Patrick, B. O.; Love, J. A. Synthesis of 2-Nickela(II)oxetanes from Nickel(0) and Epoxides: Structure, Reactivity, and a New Mechanism of Formation. *J. Am. Chem. Soc.* **2015**, *137*, 12748−12751.

(37) Laue, S.; Greiner, L.; Wöltinger, J.; Liese, A. Continuous Application of Chemzymes in a Membrane Reactor: Asymmetric Transfer Hydrogenation of Acetophenone. *Adv. Synth. Catal.* **2001**, *343* (6−7), 711−720.

(38) Schaufelberger, F.; Ramström, O. Dynamic covalent organocatalysts discovered from catalytic systems through rapid deconvolution screening. *Chem. - Eur. J.* **2015**, *21*, 12735−12740.

(39) Schenkel, L. B.; Ellman, J. A. Novel Sulfinyl Imine Ligands for Asymmetric Catalysis. *Org. Lett.* **2003**, *5* (4), 545−548.

(40) Okuda, J.; Eberle, T.; Spaniol, T. P.; Piquet-Fauré, V. Complexes of titanium and zirconium containing a tridentate linked amido−cyclopentadienyl ligand with a soft donor group: synthesis, structure, and ethylene polymerization catalysis. *J. Organomet. Chem.* **1999**, *591*, 127−137.

DOI: 10.1021/acs.inorgchem.8b01478
Inorg. Chem. 2018, 57, 10846−10856